PREDICTION OF THE THERMAL BEHAVIOR OF A PARTICULATE SPHERICAL FUEL ELEMENT USING GITT

C. V. Pessoa, pessoapen@gmail.com
Technological Center of the Army
Department of Science and Technology
Brazilian Army
Ministry of Defense
Av. das Americas, 28705, Rio de Janeiro, 23020-470, Brazil

Claudio L. de O., d7luiz@ime.eb.br
Engineering Military Institute
Department of Science and Technology
Brazilian Army
Ministry of Defense
Pr. General Tiburcio 80, Rio de Janeiro, 22290-270, Brazil

S. Jian , sujian@con.ufrj.br
Nuclear Engineering Program, COPPE
Universidade Federal do Rio de Janeiro
C.P. 68509, Rio de Janeiro, 21945-970, Brazil

Abstract. *In this work, the transient and steady state heat conduction in a spherical fuel element of a pebble-bed high temperature were studied. This pebble element is composed by a particulate region with spherical inclusions, the fuel UO_2 particles, dispersed in a graphite matrix. A convective heat transfer by helium occurs on the outer surface of the fuel element. The two-energy equation model for the case of pure conduction was applied to this particulate spherical element, generating two macroscopic temperatures, respectively, of the inclusions and of the matrix. The transient analysis was carried out by using the Generalized Integral Transform Technique (GITT) that requires low computational efforts and allows a fast evaluation of the two macroscopic transient temperatures of the particulate region. The solution by GITT leads to a system of ordinary differential equations with the unknown transformed potentials. The mechanical properties (thermal conductivity and specific heat) of the materials were supposed not to depend on the temperature and to be uniform in each region.*

Keywords: *GITT, transient and steady state heat conductions, spherical fuel element, pebble-bed reactor, two-energy equation model*

1. INTRODUCTION

The high temperature gas-cooled reactors (HTGR) appear as a promising source of energy that meets the needs of the society of 21st century, because they have the ability to offer energy at high temperatures for the generation of electricity and for industrial applications involving heat, as the production of hydrogen, with a high degree of confidence (that is itself important and also very requested by public opinion) and with competitive installation, operation and maintenance costs, compared with other main sources of energy.

The transient heat conduction analysis of the spherical fuel element of a pebble-bed reactor, a type of HTGR, is very important for its safety, because the fuel particle temperatures can't be higher than 1650^{o}C, when the leakage of fission radionuclides occurs. For this reason, this work simulates the accident of helium flow rate loss (LOFA) through the core, accompanied by reactor shutdown, predicting the transient thermal behavior of a fuel pebble element, supposed initially at a stationary operation temperature distribution.

Since the pebble is composed of 15000 fuel particles dispersed in a graphite matrix, its heat conduction analysis becomes difficult, when using just the microscopic energy equations of the two regions. One method that stands out in the solution of problems of heat conduction in heterogeneous environment with two regions is the volume average or the two-energy equation one (Hsu,1999, and Nakayama et al.,2001). Thus, by applying the average volume over a representative elementary volume REV (Fig. 1) on these microscopic equations, macroscopic equations defined in the entire domain of study are obtained, including simultaneously the two regions, and not only each region separately, as happen with the microscopic analysis.

So, once the macroscopic energy equations were obtained, the Generalized Integral Transform Technique (GITT) was applied, a hybrid numerical-analytical computational approach for convection-diffusion phenomena simulation (Cotta and Mikhailov, 1997, Ribeiro, Cotta and Mikhailov, 1993). Its hybrid feature allows the study of multi-dimensional problems with little additional computational efforts in comparison with the uni-dimensional problems, because the analytical part of the solution is applied to all independent variables unless one, converting its numerical part into the resolution of a system of ordinary differential equations with a single coordinate.

In pebble-bed high temperature reactors, the pebble fuel element usually has the diameter equal to 6cm (IAEA,2001, and Reitsma et al., 2006) and a graphite coating with a 0.5cm thickness, but here it's supposed to have no coating and the diameter equal to 5cm. Also, the cooling gas is commonly the chemically inert helium, whose temperature varies, in the Japanese High Temperature Engineering Test Reactor (HTTR), at full-power operation condition, from 950^{o}C to 395^{o}C (IAEA,2003). Here, the helium gas is supposed at a constant temperature of 672.5^{o}C during the entire transient. It was adopted too a 0.77mm fuel particle diameter, similar to the one used by the USA's Department of Energy Advanced Gas Reactor (AGR) program (Miller, Petti and Maki, 2004 and 2006). Usually, the pebble-bed high temperature reactor fuel TRISO particle is composed by an UO_2 fuel kernel, a low-density pyrolytic carbon buffer layer, a inner high-density pyrolytic carbon layer (I-PyC), a silicon carbide layer (SiC) and a outer high-density pyrolytic carbon layer (O-PyC), but in this work it was assumed the simplification of an one-region UO_2 fuel particle. The mechanical properties (thermal conductivity and specific heat) of both materials (UO_2 and graphite) were supposed not to depend on the temperature and to be uniform in each region.

2. MATHEMATICAL FORMULATION

The microscopic energy equations of a two-region pebble fuel element and its interfacial equations are, respectively:

$$\rho_f c_{pf}\frac{\partial T_f}{\partial t} = \nabla.\left(k_f \nabla T_f\right) \qquad \rho_s c_{ps}\frac{\partial T_s}{\partial t} = \nabla.\left(k_s \nabla T_s\right) + g_s(t) \tag{1}$$

$$T_f = T_s \qquad k_f \nabla T_f = k_s \nabla T_s, \tag{2}$$

where it was considered the perfect thermal contact between the two regions and where T_j is the microscopic temperature of the region j, subscripts f and s denote, respectively, graphite and UO_2 regions, ρ is the density, c_p, the specific heat, k, the thermal conductivity, and $g_s(t)$, the volumetric heat generation rate of the UO_2 region.

Applying the two-energy equation model for the case of pure conduction, Hsu (1999) showed that the energy Eqs. (1), averaged over a representative elementary volume REV (Fig. 1), whose length scale ℓ is presumed to be much larger than the fuel particle diameter d_P, become:

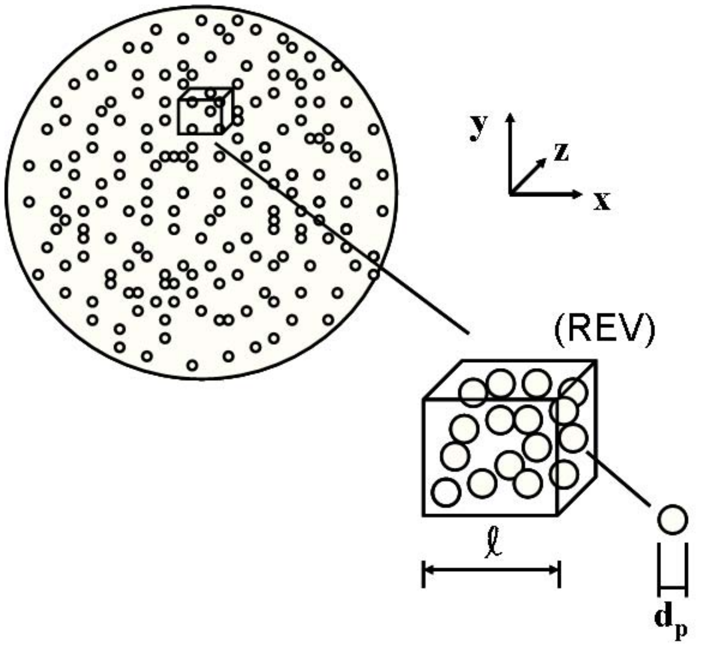

Figure 1: Schematic representation of the spherical fuel element and its representative elementary volume REV

$$\rho_f c_{pf}\frac{\partial\left(\phi\left\langle T_f\right\rangle^i\right)}{\partial t} = \bar{\nabla}.\left[k_f\bar{\nabla}\left(\phi\left\langle T_f\right\rangle^i\right)\right] + \bar{\nabla}.k_f G\left(\bar{\nabla}\left\langle T_f\right\rangle^i - \sigma\bar{\nabla}\left\langle T_s\right\rangle^i\right) + h_{fs}a_{fs}\left(\left\langle T_s\right\rangle^i - \left\langle T_f\right\rangle^i\right) \tag{3}$$

$$\rho_s c_{ps}\frac{\partial\left[(1-\phi)\left\langle T_s\right\rangle^i\right]}{\partial t} = \bar{\nabla}.\left[k_s\bar{\nabla}\left((1-\phi)\left\langle T_s\right\rangle^i\right)\right] - \bar{\nabla}.k_s G\left(\bar{\nabla}\left\langle T_f\right\rangle^i - \sigma\bar{\nabla}\left\langle T_s\right\rangle^i\right) - h_{fs}a_{fs}\left(\left\langle T_s\right\rangle^i - \left\langle T_f\right\rangle^i\right) +$$

$$+ (1-\phi)\, g_s(t) \qquad (4)$$

where ϕ is the porosity, $\langle T_j \rangle^i$ is the intrinsic volume average temperature of the region j over the REV, G is the thermal tortuosity parameter, h_{fs}, the interfacial heat transfer coefficient, a_{fs}, the specific interfacial area, and $\bar{\nabla}$, the macroscopic gradient operator. Supposing that the problem is one-dimensional, and that ϕ, G and k_j are uniform and ϕ is constant, Eqs. (3) and (4) become:

$$\phi \frac{\partial \langle T_f \rangle^i}{\partial t} = (\phi + G)\alpha_f \frac{1}{r}\frac{\partial^2 (r \langle T_f \rangle^i)}{\partial r^2} + \frac{a_{fs}h_{fs}}{\rho_f c_{pf}}\left(\langle T_s \rangle^i - \langle T_f \rangle^i \right) - \sigma G \alpha_f \frac{1}{r}\frac{\partial^2 (r \langle T_s \rangle^i)}{\partial r^2} \qquad (5)$$

$$(1-\phi)\frac{\partial \langle T_s \rangle^i}{\partial t} = (1-\phi+\sigma G)\alpha_s \frac{1}{r}\frac{\partial^2 (r \langle T_s \rangle^i)}{\partial r^2} - \frac{a_{fs}h_{fs}}{\rho_s c_{ps}}\left(\langle T_s \rangle^i - \langle T_f \rangle^i \right) - \alpha_s G \frac{1}{r}\frac{\partial^2 (r \langle T_f \rangle^i)}{\partial r^2} + \frac{(1-\phi) g_s(t)}{\rho_s c_{ps}}, \qquad (6)$$

for $0 < r < r_P$ and $t > 0$, where r_P is the radius of the pebble, α, the thermal diffusivity, and $\sigma \equiv k_s/k_f$. Defining the following adimensional groups:

$$R = \frac{r}{r_P} \qquad \tau = \frac{\alpha_f\, t}{r_P^2} \qquad \theta_j = \left.\frac{\langle T_j \rangle^i - T_\infty}{T_0 - T_\infty}\right]_{j=s,f} \qquad \delta = \frac{\alpha_s}{\alpha_f} \qquad \Phi_s = \frac{r_P^2\, g_s(t)}{k_f\,(T_0 - T_\infty)}, \qquad (7)$$

where T_∞ is the surrounding helium gas constant temperature and T_0 is a reference temperature, Eqs. (5) and (6) become, respectively:

$$\phi \frac{\partial \theta_f}{\partial \tau} = (\phi + G)\frac{1}{R}\frac{\partial^2 (R\theta_f)}{\partial R^2} + \frac{a_{fs}h_{fs}r_P^2}{k_f}(\theta_s - \theta_f) - \sigma G \frac{1}{R}\frac{\partial^2 (R\theta_s)}{\partial R^2} \qquad (8)$$

$$(1-\phi)\frac{\partial \theta_s}{\partial \tau} = (1-\phi+\sigma G)\delta \frac{1}{R}\frac{\partial^2 (R\theta_s)}{\partial R^2} - \frac{a_{fs}h_{fs}\delta r_P^2}{k_f \sigma}(\theta_s - \theta_f) - \delta G \frac{1}{R}\frac{\partial^2 (R\theta_f)}{\partial R^2} + \frac{(1-\phi)\Phi_s(\tau)\delta}{\sigma}, \qquad (9)$$

for $0 < R < 1$. Multiplying Eqs. (8) and (9) by R and introducing the following transformation of variables:

$$\theta_f(R,\tau) = \frac{U_f(R,\tau)}{R} \quad \text{and} \quad \theta_s(R,\tau) = \frac{U_s(R,\tau)}{R}, \quad \text{they turn to:} \qquad (10)$$

$$\phi \frac{\partial U_f}{\partial \tau} = (\phi + G)\frac{\partial^2 U_f}{\partial R^2} + \frac{a_{fs}h_{fs}r_P^2}{k_f}(U_s - U_f) - \sigma G \frac{\partial^2 U_s}{\partial R^2} \qquad (11)$$

$$(1-\phi)\frac{\partial U_s}{\partial \tau} = (1-\phi+\sigma G)\delta \frac{\partial^2 U_s}{\partial R^2} - \frac{a_{fs}h_{fs}\delta r_P^2}{k_f \sigma}(U_s - U_f) - \delta G \frac{\partial^2 U_f}{\partial R^2} + \frac{(1-\phi)\Phi_s(\tau)\delta}{\sigma} R \qquad (12)$$

Dividing Eqs. (11) and (12), respectively, by ϕ and $(1-\phi)$ and defining the following groups of parameters:

$$A = \frac{(\phi + G)}{\phi} \quad B = \frac{a_{fs}h_{fs}r_P^2}{\phi\, k_f} \quad C = -\frac{\sigma G}{\phi} \quad D = \frac{(1-\phi+\sigma G)\delta}{(1-\phi)} \qquad (13)$$

$$E = -\frac{a_{fs}h_{fs}\delta r_P^2}{(1-\phi)\, k_f \sigma} \quad F = -\frac{\delta G}{(1-\phi)} \quad G^*(\tau) = \frac{\Phi_s(\tau)\delta}{\sigma}, \quad \text{Eqs. (11) and (12) become:} \qquad (14)$$

$$\frac{\partial U_f}{\partial \tau} = A\frac{\partial^2 U_f}{\partial R^2} + B(U_s - U_f) + C\frac{\partial^2 U_s}{\partial R^2} \qquad (15)$$

$$\frac{\partial U_s}{\partial \tau} = D\frac{\partial^2 U_s}{\partial R^2} + E(U_s - U_f) + F\frac{\partial^2 U_f}{\partial R^2} + G^*(\tau)R, \quad \text{with the respective convective boundary conditions:} \qquad (16)$$

$$\frac{\partial U_f(1,\tau)}{\partial R} + S^*\, U_f(1,\tau) = 0 \quad \text{and} \qquad (17)$$

$$\frac{\partial U_s(1,\tau)}{\partial R} + W^*\, U_s(1,\tau) = 0, \quad \text{where} \quad S^* \equiv Bi_f - 1, \quad W^* \equiv Bi_s - 1 \quad \text{and the Biot numbers are:} \qquad (18)$$

$$Bi_f = \frac{h_{He} r_P}{k_f} \quad \text{and} \quad Bi_s = \frac{h_{He} r_P}{k_s}, \quad \text{where } h_{He} \text{ is the helium heat transfer coefficient.} \qquad (19)$$

Also, for $R = 0$, the boundary conditions are:

$$U_f(0,\tau) = 0 \quad \text{and} \quad U_s(0,\tau) = 0, \quad \text{because} \quad [U_f(R,\tau) = R\theta_f(R,\tau)]_{R=0} = 0\;\theta_f(0,\tau) = 0, \tag{20}$$

and similarly for U_s.

To get the initial conditions $U_f(R,0)$ and $U_s(R,0)$, the following stationary problem must be solved for $U_{fs}(R)$ and $U_{ss}(R)$:

$$0 = A\frac{d^2U_{fs}}{dR^2} + B(U_{ss} - U_{fs}) + C\frac{d^2U_{ss}}{dR^2} \tag{21}$$

$$0 = D\frac{d^2U_{ss}}{dR^2} + E(U_{ss} - U_{fs}) + F\frac{d^2U_{fs}}{dR^2} + \; G_s^*R, \tag{22}$$

for $0 < R < 1$, with the same original boundary conditions, Eqs. (17), (18) and (20), and where G_s^*, in this case, is not dependent on time. So the initial conditions $U_f(R,0)$ and $U_s(R,0)$ are:

$$U_f(R,0) = U_{fs}(R) \quad \text{and} \quad U_s(R,0) = U_{ss}(R) \tag{23}$$

For solving the system of partial differential equations, Eqs. (15) to (20) more Eqs. (23), the following associated Sturm-Liouville problem are adopted:

$$\frac{d^2\psi_{1i}(R)}{dR^2} + \mu_1^2\psi_{1i}(R) = 0, \quad \text{em} \quad 0 < R < 1 \tag{24}$$

$$\psi_{1i}(0) = 0 \tag{25}$$

$$\frac{d\psi_{1i}(1)}{dR} + S^*\psi_{1i}(1) = 0, \tag{26}$$

$$\frac{d^2\psi_{2i}(R)}{dR^2} + \mu_2^2\psi_{2i}(R) = 0, \quad \text{em} \quad 0 < R < 1 \tag{27}$$

$$\psi_{2i}(0) = 0 \tag{28}$$

$$\frac{d\psi_{2i}(1)}{dR} + W^*\psi_{2i}(1) = 0, \tag{29}$$

whose solutions (eigenfunctions, eigenvalues and norms), are, respectively:

$$\psi_{1i}(R) = sin\mu_{1i}R \qquad \psi_{2i}(R) = sin\mu_{2i}R \tag{30}$$

$$\mu_{1i}\;cot\mu_{1i} = -S^* \qquad \mu_{2i}\;cot\mu_{2i} = -W^* \tag{31}$$

$$N_{1i}(\mu_{1i}) = \int_0^1 \psi_{1i}^2(\mu_{1i},R)dR = \frac{\mu_{1i}^2 + S^{*2} + S^*}{2(\mu_{1i}^2 + S^{*2})} \qquad N_{2i}(\mu_{2i}) = \int_0^1 \psi_{2i}^2(\mu_{2i},R)dR = \frac{\mu_{2i}^2 + W^{*2} + W^*}{2(\mu_{2i}^2 + W^{*2})}, \tag{32}$$

for $i = 1, 2, 3, ...$ Defining now the integral transform functions $\overline{U}_{fi}(\tau)$ and $\overline{U}_{si}(\tau)$, such that:

$$U_f(R,\tau) \equiv \sum_{i=1}^{\infty} \frac{\psi_{1i}(\mu_{1i},R)\overline{U}_{fi}(\tau)}{N_{1i}^{1/2}}, \quad \text{and} \tag{33}$$

$$U_s(R,\tau) \equiv \sum_{i=1}^{\infty} \frac{\psi_{2i}(\mu_{2i},R)\overline{U}_{si}(\tau)}{N_{2i}^{1/2}}, \tag{34}$$

it's possible to prove, because of the orthogonality property of the eigenfunctions ψ_{1i} e ψ_{2i}, that:

$$\overline{U}_{fi}(\tau) = \frac{1}{N_{1i}^{1/2}} \int_0^1 \psi_{1i}(\mu_{1i},R)U_f(R,\tau)dR \tag{35}$$

$$\overline{U}_{si}(\tau) = \frac{1}{N_{2i}^{1/2}} \int_0^1 \psi_{2i}(\mu_{2i},R)U_s(R,\tau)dR \tag{36}$$

The next step is to perform the integral transformation of the partial differential Eqs. (15) and (16), in order to reduce them into an ordinary differential system. So the operators:

$$\frac{1}{N_{1i}^{1/2}}\int_0^1 \psi_{1i} dR \quad \text{and} \quad \frac{1}{N_{2i}^{1/2}}\int_0^1 \psi_{2i} dR \quad \text{are respectively applied to Eqs. (15) and (16) to find:} \tag{37}$$

$$\frac{d\overline{U}_{fi}}{dt} + A\mu_{1i}^2 \overline{U}_{fi} = \frac{A}{N_{1i}^{1/2}}\left(\psi_{1i}(1)\frac{\partial U_f(1,\tau)}{\partial R} - U_f(1,\tau)\frac{d\psi_{1i}(1)}{dR}\right) + \frac{C}{N_{1i}^{1/2}}\int_0^1 \psi_{1i}\frac{\partial^2 U_s}{\partial R^2}dR +$$

$$+\frac{B}{N_{1i}^{1/2}}\int_0^1 \psi_{1i} U_s dR - \frac{B}{N_{1i}^{1/2}}\int_0^1 \psi_{1i} U_f dR \tag{38}$$

$$\frac{d\overline{U}_{si}}{dt} + D\mu_{2i}^2 \overline{U}_{si} = \frac{D}{N_{2i}^{1/2}}\left(\psi_{2i}(1)\frac{\partial U_s(1,\tau)}{\partial R} - U_s(1,\tau)\frac{d\psi_{2i}(1)}{dR}\right) + \frac{F}{N_{2i}^{1/2}}\int_0^1 \psi_{2i}\frac{\partial^2 U_f}{\partial R^2}dR +$$

$$+\frac{E}{N_{2i}^{1/2}}\int_0^1 \psi_{2i} U_s dR - \frac{E}{N_{2i}^{1/2}}\int_0^1 \psi_{2i} U_f dR + \frac{G^*(\tau)}{N_{2i}^{1/2}}\int_0^1 \psi_{2i} R dR. \tag{39}$$

The first term on the right hand side of Eq. (38) is evaluated as zero by applying $\int_0^1 dR$ to the subtraction of the following identities

$$\frac{\partial\left(\psi_{1i}\partial U_f/\partial R\right)}{\partial R} = \psi_{1i}\frac{\partial^2 U_f}{\partial R^2} + \frac{d\psi_{1i}}{dR}\frac{\partial U_f}{\partial R} \quad \text{and} \quad \frac{\partial\left(U_f d\psi_{1i}/dR\right)}{\partial R} = U_f\frac{d^2\psi_{1i}}{dR^2} + \frac{d\psi_{1i}}{dR}\frac{\partial U_f}{\partial R}$$

and by accounting for the boundary Eqs. (17) and (26). The second term on the right hand side of Eq. (38) is rewritten as shown below:

$$\frac{C}{N_{1i}^{1/2}}\int_0^1\left(\psi_{1i}\frac{\partial^2 U_s}{\partial R^2}\right)dR = \frac{C}{N_{1i}^{1/2}}\int_0^1\left[\psi_{1i}\frac{\partial^2 U_s}{\partial R^2} - U_s\frac{d^2\psi_{1i}}{dR^2}\right]dR + \frac{C}{N_{1i}^{1/2}}\int_0^1 U_s\frac{d^2\psi_{1i}}{dR^2}dR, \tag{40}$$

where the first term on the right hand side is solved by applying $\int_0^1 dR$ to the subtraction of the following identities

$$\frac{\partial\left(\psi_{1i}\partial U_s/\partial R\right)}{\partial R} = \psi_{1i}\frac{\partial^2 U_s}{\partial R^2} + \frac{d\psi_{1i}}{dR}\frac{\partial U_s}{\partial R} \quad \text{and} \quad \frac{\partial\left(U_s d\psi_{1i}/dR\right)}{\partial R} = U_s\frac{d^2\psi_{1i}}{dR^2} + \frac{d\psi_{1i}}{dR}\frac{\partial U_s}{\partial R}$$

and by accounting for the boundary conditions of the second of the Eqs. (20) and of the Eq. (25), while the second integral on the right hand side of Eq.(40) is evaluated by substituting the inverse formula, Eq.(34), for $U_s(R,\tau)$, and Eq.(24) for $d^2\psi_{1i}/dR^2$, to find:

$$\frac{C}{N_{1i}^{1/2}}\int_0^1\left(\psi_{1i}\frac{\partial^2 U_s}{\partial R^2}\right)dR = \frac{C}{N_{1i}^{1/2}}\left[\psi_{1i}(1)\frac{\partial U_s(1,\tau)}{\partial R} - U_s(1,\tau)\frac{d\psi_{1i}(1)}{dR}\right] + \sum_{j=1}^{\infty} B_{ij}^*\overline{U}_{sj} =^a$$

$$= \frac{C}{N_{1i}^{1/2}}\left(S^* - W^*\right)\psi_{1i}(1)U_s(1,\tau) + \sum_{j=1}^{\infty} B_{ij}^*\overline{U}_{sj} =^b \sum_{j=1}^{\infty} A_{ij}^*\overline{U}_{sj} + \sum_{j=1}^{\infty} B_{ij}^*\overline{U}_{sj}, \quad \text{where} \tag{41}$$

$$A_{ij}^* = \frac{C\left(S^* - W^*\right)}{N_{1i}^{1/2}N_{2j}^{1/2}}\psi_{1i}(1)\psi_{2j}(1), \quad B_{ij}^* = \frac{-C\mu_{1i}^2}{N_{1i}^{1/2}N_{2j}^{1/2}}\int_0^1 \psi_{1i}\psi_{2j} dR,$$

where the boundary conditions of Eqs.(18) and (26) were used in equality (a) and the inverse formula of Eq.(34) was used in equality (b).

Similarly the third term on the right hand side of Eq. (38) is evaluated as

$$\frac{B}{N_{1i}^{1/2}}\int_0^1 \psi_{1i} U_s dR = \sum_{j=1}^{\infty} D_{ij}^*\overline{U}_{sj}, \quad \text{where Eq. (34) was used and} \quad D_{ij}^* = \frac{B}{N_{1i}^{1/2}N_{2j}^{1/2}}\int_0^1 \psi_{1i}\psi_{2j} dR, \tag{42}$$

and the fourth term on the right hand side of Eq. (38) is evaluated as

$$\frac{-B}{N_{1i}^{1/2}}\int_0^1 \psi_{1i}U_f dR = \frac{-B}{N_{1i}^{1/2}}\sum_{j=1}^{\infty}\frac{1}{N_{1j}^{1/2}}\left[\int_0^1 \psi_{1i}\psi_{1j}dR\right]\overline{U}_{fj} = -B\overline{U}_{fi}, \quad \text{where Eq. (33) and} \tag{43}$$

the orthogonality of the eigenfunctions ψ_{1i} of the Sturm-Liouville problem defined by Eqs. (24) to (26) were used.

Now Eqs. (41), (42) and (43) are substituted in Eq. (38) to find:

$$\frac{d\overline{U}_{fi}}{dt} + A\mu_{1i}^2\overline{U}_{fi} = \sum_{j=1}^{\infty}A_{ij}^*\overline{U}_{sj} + \sum_{j=1}^{\infty}B_{ij}^*\overline{U}_{sj} + \sum_{j=1}^{\infty}D_{ij}^*\overline{U}_{sj} - B\overline{U}_{fi} \quad \text{or}$$

$$\frac{d\overline{U}_{fi}}{d\tau} + (A\mu_{1i}^2 + B)\overline{U}_{fi} - \sum_{j=1}^{\infty}E_{ij}^*\overline{U}_{sj} = 0, \quad \text{where} \quad E_{ij}^* = A_{ij}^* + B_{ij}^* + D_{ij}^* \tag{44}$$

Similar development of Eq.(39) leads to:

$$\frac{d\overline{U}_{si}}{d\tau} + (D\mu_{2i}^2 - E)\overline{U}_{si} - \sum_{j=1}^{\infty}F_{ij}^*\overline{U}_{fj} - H_i^*G^*(\tau) = 0, \text{ where } \quad F_{ij}^* = I_{ij}^* + J_{ij}^* + L_{ij}^*, \tag{45}$$

$$I_{ij}^* = \frac{F\,(W^* - S^*)}{N_{2i}^{1/2}N_{1j}^{1/2}}\psi_{2i}(1)\psi_{1j}(1), \quad J_{ij}^* = \frac{-F\mu_{2i}^2}{N_{2i}^{1/2}N_{1j}^{1/2}}\int_0^1 \psi_{2i}\psi_{1j}dR, \quad L_{ij}^* = \frac{-E}{N_{2i}^{1/2}N_{1j}^{1/2}}\int_0^1 \psi_{2i}\psi_{1j}dR \tag{46}$$

$$\text{and} \quad H_i^* = \frac{1}{\mu_{2i}N_{2i}^{1/2}}\left(\frac{\sin\mu_{2i}}{\mu_{2i}} - \cos\mu_{2i}\right), \quad \text{which} \tag{47}$$

is obtained by applying the second of the operators (37) to the fourth term on the right hand side of Eq. (16), as follows:

$$\frac{1}{N_{2i}^{1/2}}\int_0^1 \psi_{2i}G^*(\tau)RdR = \frac{G^*(\tau)}{N_{2i}^{1/2}}\int_0^1 \psi_{2i}RdR = \frac{G^*(\tau)}{\mu_{2i}N_{2i}^{1/2}}\left(\frac{\sin\mu_{2i}}{\mu_{2i}} - \cos\mu_{2i}\right) = H_i^*G^*(\tau) \tag{48}$$

Then the number of eigenfunctions ψ_{1i} and ψ_{2i} are respectively limited to a sufficiently large order, N, for the desired tolerance in the converged potentials, so that Eqs. (44) and (45) generate the following O.D.E. system:

$$\{y'(\tau)\} + [M]\{y(\tau)\} = \{P\}G^*(\tau), \quad \text{where} \quad \{y(\tau)\} = \left[\overline{U}_{f1}(\tau), ..., \overline{U}_{fN}(\tau), \overline{U}_{s1}(\tau), ..., \overline{U}_{sN}(\tau)\right]^T, \tag{49}$$

$$\{P\} = [\underbrace{0,\ ...\ ,0}_{N},\ H_1^*, ..., H_N^*\ ]^T, \tag{50}$$

$$[M] = \begin{pmatrix} A\mu_{11}^2 + B & 0 & \cdots & 0 & -E_{11}^* & -E_{12}^* & \cdots & -E_{1N}^* \\ 0 & A\mu_{12}^2 + B & \cdots & 0 & -E_{21}^* & -E_{22}^* & \cdots & -E_{2N}^* \\ \vdots & \vdots & \ddots & \vdots & \vdots & \vdots & \ddots & \vdots \\ 0 & 0 & \cdots & A\mu_{1N}^2 + B & -E_{N1}^* & -E_{N2}^* & \cdots & -E_{NN}^* \\ -F_{11}^* & -F_{12}^* & \cdots & -F_{1N}^* & D\mu_{21}^2 - E & 0 & \cdots & 0 \\ -F_{21}^* & -F_{22}^* & \cdots & -F_{2N}^* & 0 & D\mu_{22}^2 - E & \cdots & 0 \\ \vdots & \vdots & \ddots & \vdots & \vdots & \vdots & \ddots & \vdots \\ -F_{N1}^* & -F_{N2}^* & \cdots & -F_{NN}^* & 0 & 0 & \cdots & D\mu_{2N}^2 - E \end{pmatrix}$$

$$\text{and whose initial conditions} \quad \{y(0)\} = \left[\overline{U}_{f1}(0), ..., \overline{U}_{fN}(0), \overline{U}_{s1}(0), ..., \overline{U}_{sN}(0)\right]^T \quad \text{are} \tag{51}$$

obtained by transforming the initial condition of Eqs. (23), as follows:

$$\overline{U}_{fi}(0) = \frac{1}{N_{1i}}\int_0^1 \psi_{1i}(R)U_f(R,0)dR = \frac{1}{N_{1i}}\int_0^1 \psi_{1i}(R)\,U_{fs}(R)\,dR \tag{52}$$

$$\overline{U}_{si}(0) = \frac{1}{N_{2i}}\int_0^1 \psi_{2i}(R)U_s(R,0)dR = \frac{1}{N_{2i}}\int_0^1 \psi_{2i}(R)\,U_{ss}(R)\,dR \tag{53}$$

The ODE system solution $\{y(\tau)\}$ of Eqs. (49) and (51) provides $\overline{U}_{fi}(\tau)$ and $\overline{U}_{si}(\tau)$, which both, by means of the inverse formulae Eqs. (33) e (34), allow respectively the calculation of $U_f(R,\tau)$ and $U_s(R,\tau)$, which both, in turn, through Eqs. (10) and the third of Eqs. (7), lead respectively to $\theta_f(R,\tau)$ and $\theta_s(R,\tau)$ and, finally, to the desired potentials $\langle T_f\rangle^i(r,t)$ and $\langle T_s\rangle^i(r,t)$.

Now, the formulas for ϕ , G , a_{fs} , $g_s(t)$, g_s and h_{fs} used in this work, will be given. ϕ and a_{fs} were geometrically obtained as:

$$\phi = 1 - \frac{n_p r_{p'}^3}{r_P^3} \quad \text{and} \quad a_{fs} = 3\frac{(1-\phi)}{r_{p'}}, \quad \text{where } n_p \text{ is the number of fuel particles per fuel element} \tag{54}$$

and $r_{p'}$ is the fuel particle radius. The expression for G , presented by Hsu (1999) , is:

$$G = \frac{k_e/k_f - \phi - (1-\phi)\sigma}{(1-\sigma)^2}, \quad \text{where, despite the effective stagnant thermal conductivity, } k_e\text{ ,} \tag{55}$$

of the two-region mixture is defined under the hypothesis of local thermal equilibrium, this expression for G, according to Hsu (1999), is also valid for the non-thermal equilibrium cases, because G depends only on the local interfacial geometry and on the solid and fluid thermal properties. For the case of nontouching inclusions, Hsu (1999) presented the following expression for k_e:

$$k_e/k_f = 1 - (1-\phi)^{2/3} + \frac{\sigma(1-\phi)^{2/3}}{\sigma + (1-\sigma)(1-\phi)^{1/3}} \tag{56}$$

In this work, LOFA, accompanied by reactor shutdown, is simulated. Todreas and Kasimi (1990) showed the following expression for the decay volumetric heat generation rate after shutdown:

$$\frac{g_s(t)}{g_s/10} = \frac{1}{(t+10)^{0.2}} - \frac{0.87}{(t+2\;10^7)^{0.2}} - \frac{1}{(t+t_0+10)^{0.2}} + \frac{0.87}{(t+t_0+2\;10^7)^{0.2}}, \tag{57}$$

where t is the time (s) after shutdown and t_0 is the period of time during which the reactor operated at a constant power level, before the beginning of the shutdown, and g_s is the stationary operating volumetric heat generation rate, which is given by:

$$g_s = \frac{P_P}{n_p\;4/3\;\pi r_p^3}, \quad \text{where } P_P \text{ is the average stationary operating output power per fuel element.} \tag{58}$$

For h_{fs}, the expression obtained by Kuwahara, Shirota and Nakayama (2001) was used here for the asymptotic case of no fluid flow, i.e., for the Reynolds number equal to zero, leading to:

$$\frac{2h_{fs}r_{p'}}{k_f} = 1 + \left(\frac{4(1-\phi)}{\phi}\right), \quad \text{valid for } 0.2 < \phi < 0.9. \tag{59}$$

3. RESULTS AND DISCUSSION

Table 1: Physical or design parameters

k_{UO2}	(W/m K)	2.23	k_{graph}	(W/m K)	41.55
ρ_{UO2}	(g/cm^3)	10.4	ρ_{Graph}	(g/cm^3)	1.75
c_{pUO2}	(J/kgK)	350 (1)	c_{pGraph}	(J/kgK)	1976 (1)
P_P (2)	(kW)	0.881 (3)	t_0	(ano)	1

(1) - at 1400^{o}C *(2)* - the average stationary operating output power per fuel element *(3)* - (Zhang et al., 2006)

Table 1 shows some physical or design parameters used in the simulation. The fuel pebble element is supposed initially at a stationary operation temperature distribution, with $h_{He} = 120W/m^2K$. After the beginning of the LOFA, natural convection heat transfer through helium occurs, with h_{He} supposed equal to $30W/m^2K$.

To get the initial conditions $U_f(R,0)$ and $U_s(R,0)$ of the transient problem composed by Eqs. (15) to (20) more Eqs. (23), the stationary problem of the Eqs. (21) and (22), with the boundary conditions of Eqs. (17), (18) and (20), was analytically solved for $U_{fs}(R)$ and $U_{ss}(R)$, with the help of the Mathematica program. The intrinsic average stationary temperature profiles, as a function of the radial coordinate, were obtained, for $h_{fs} = 66000W/m^2K$, achieved through Eq.(59), and for $h_{He} = 30W/m^2K$ (Fig. 2). Figure 3 show their details around the external surface. It can be observed that:

1. the temperatures of both regions decline, as expected, from the center to the surface of the spherical fuel element;

2. the temperatures of both regions are very close to one another;

3. the UO_2 temperatures are higher than the graphite ones, as expected because the UO_2 region generates heat, except near the outer surface, where the situation is reversed;

4. the UO_2 temperatures remain below the tolerable limit of 1650^oC for the fuel particles.

Considering now the simulation of transient thermal behavior, using the Mathematica program and choosing $N = 10$, respectively, for the numbers of eigenfunctions ψ_{1i} and ψ_{2i}, the constant coefficient O.D.E. system of Eqs. (49) and (51) was obtained and solved for $\overline{U}_{fi}(\tau)$ e $\overline{U}_{si}(\tau)$, leading, through Eqs. (33) and (34), to $U_f(R,\tau)$ and $U_s(R,\tau)$ and also to the desired potentials $\langle T_f \rangle^i (r,t)$ and $\langle T_s \rangle^i (r,t)$, through Eqs. (10) and the third of Eqs. (7). The processing time of the computer program was 4s, for an Intel Pentium 4HT 3.0GHz computer with RAM memory of 512MB. The intrinsic average transient temperature profiles as a function of the radial coordinate and the time are shown in Figs. 4 and 5. It can be observed that:

1. as expected, the temperatures of both regions decline from the stationary initial temperatures to the constant temperature of the surrounding helium of 672.5^oC;

2. comparing Figs. 4 and 5, again the temperatures of both regions are very close to one another and again the UO_2 temperatures are higher than the graphite ones;

3. both volume average temperatures over the spherical fuel element, $\langle T_f \rangle^i_{avg}(t)$ and $\langle T_s \rangle^i_{avg}(t)$, reach about 725.5^oC in 90 minutes. Here the definitions of the volume averages over the fuel element of the intrinsic volume average temperatures over the REV were used and are:

$$\langle T_f \rangle^i_{avg}(t) \equiv \frac{3}{r_P^2} \int_0^{r_P} r^2 \langle T_f \rangle^i (r,t)\, dr \qquad \text{and} \qquad \langle T_s \rangle^i_{avg}(t) \equiv \frac{3}{r_P^2} \int_0^{r_P} r^2 \langle T_s \rangle^i (r,t)\, dr \tag{60}$$

The intrinsic temperatures of both regions are very close to each other, probably because the value of $h_{fs} = 66000 W/m^2K$ is very high, facilitating the heat exchange between the two regions.

Near the outer surface, the graphite temperatures are higher than the UO_2 ones, because the temperatures of the two regions are very close to one another and because the UO_2 thermal conductivity is much smaller than the graphite one, which makes the radial gradient of $\langle T_s \rangle^i$, at the external boundary surface, much higher, in absolute values, than the $\langle T_f \rangle^i$'s one, as can be seen by examining Eqs. (17) and (18).

It should be mentioned that Eq. (59) was supposed to be approximately valid in this work, even though the porosity ϕ for the considered physical problem, equal to 0.95, is out of the range of validity of this equation.

4. CONCLUSIONS

In this work, the transient and steady state heat conduction analyses in a pebble-bed reactor particulate fuel element, using the two-energy equation model, were carried out. The solutions of the stationary problem were utilized as the initial conditions for the transient one, for which GITT was applied. The results showed consistency and the processing time of the computer program was only 4s, confirming, as expected, the low computational costs of the utilization of GITT.

The next steps for this work may be the comparison of these results, using GITT, with those of another method, as the finite difference method, and, to improve the results of Fig. 3, the following boundary condition could be utilized:

$$U_s(1,\tau) = U_f(1,\tau), \quad \text{which is equivalent to} \quad \langle T_s \rangle^i (r_P,t) = \langle T_f \rangle^i (r_P,t), \tag{61}$$

instead of the convective boundary condition of Eq.(18). The condition of Eq. (61) is better than the one of Eq.(18), because the fuel particles actually doesn't contact too much the outer surface of the fuel element and, consequently, the helium gas.

5. ACKNOWLEDGEMENTS

The authors are grateful to the Brazilian National Research Council (MCT/ CNPq), the Ministry of Education of Brazil (MEC/CAPES), the Ministry of Defense of Brazil (MD), particularly the Technological Center of the Army (CTEx), and the Funding Agency of the State of Rio de Janeiro (FAPERJ) for the financial support during the realization of the work.

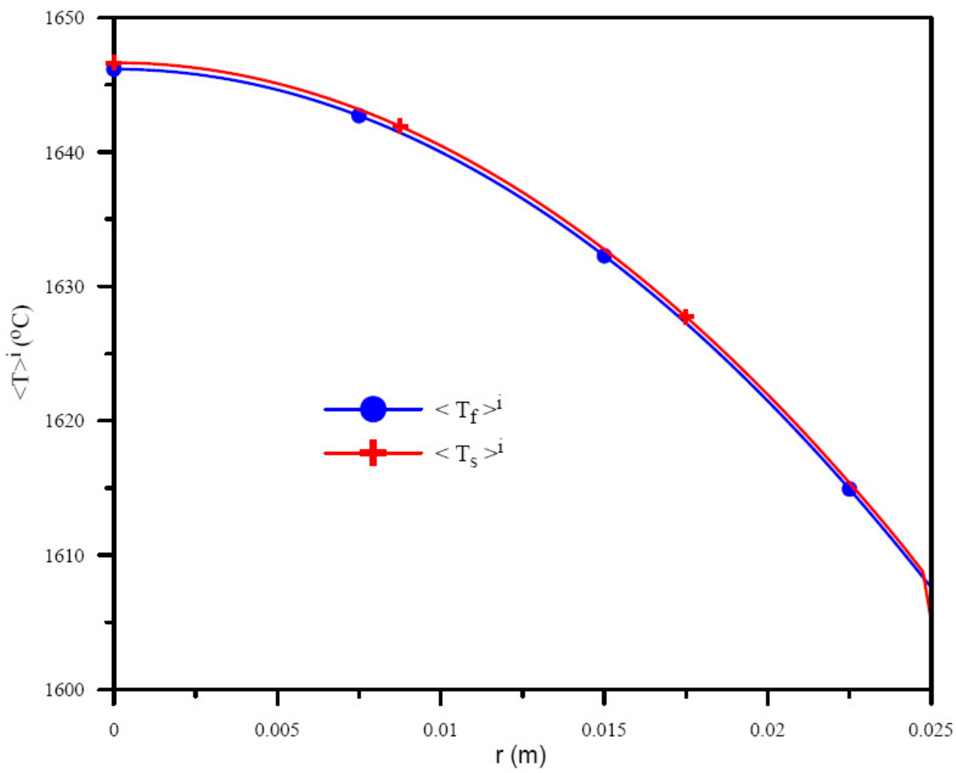

Figure 2: $\langle T_{fs}\rangle^i(r)$ and $\langle T_{ss}\rangle^i(r)$ for $h_{fs} = 66000W/m^2K$ and for $h_{He} = 120W/m^2K$

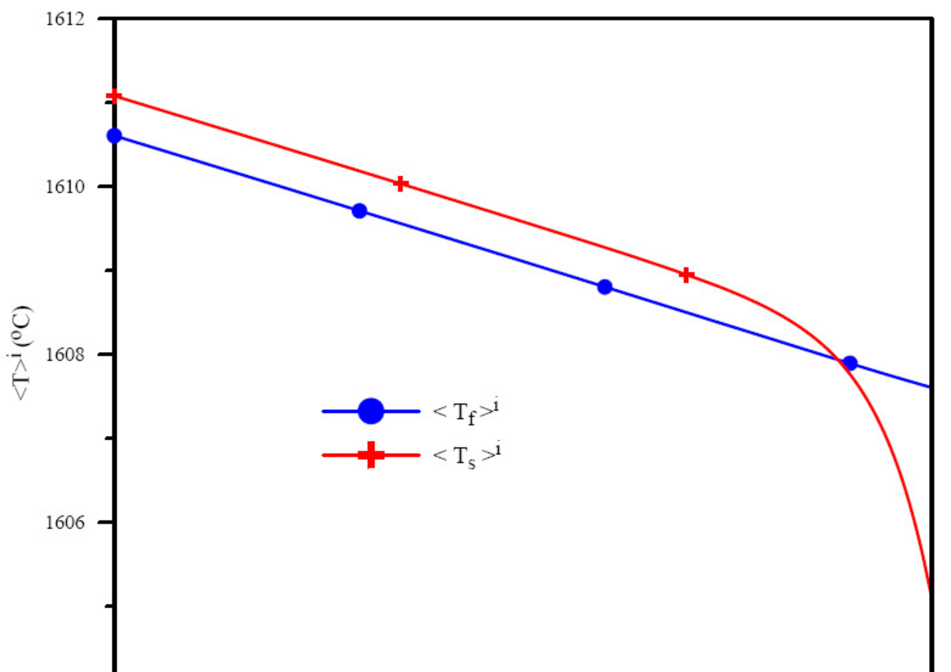

Figure 3: Detail of Fig. 2 around the external surface

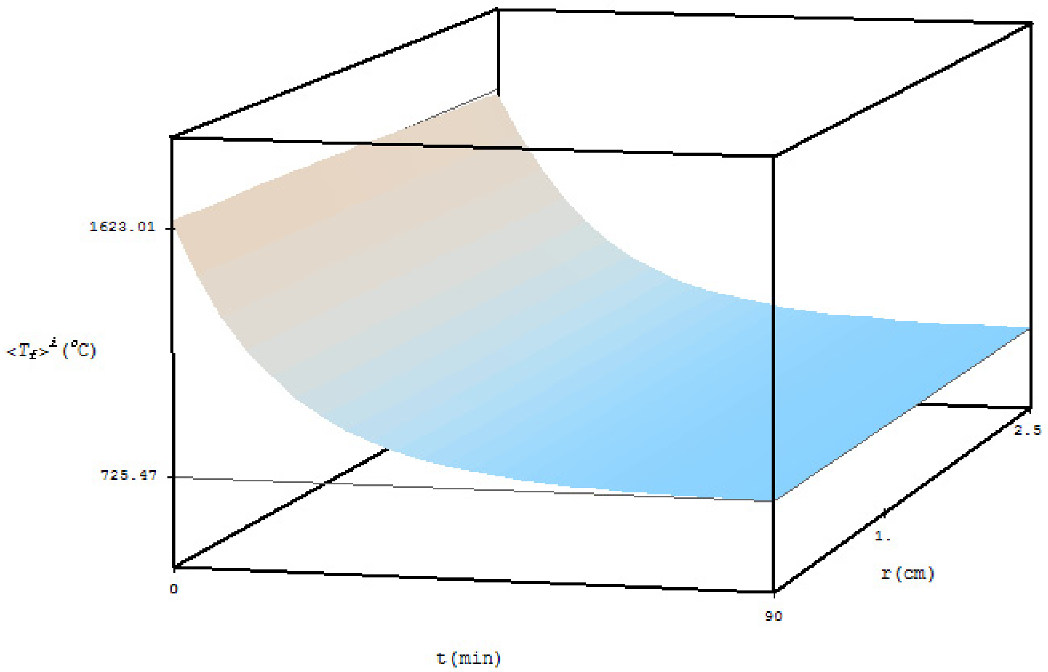

Figure 4: $\langle T_f \rangle^i(r,t)$ for $h_{fs} = 66000 W/m^2K$ and for $h_{He} = 30 W/m^2K$

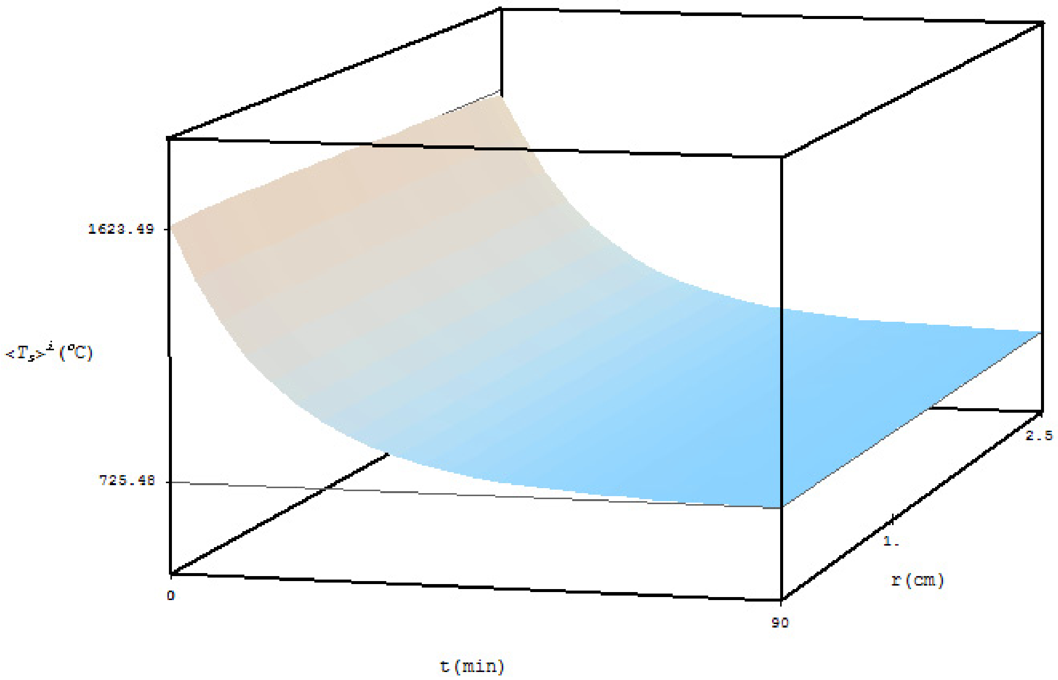

Figure 5: $\langle T_s \rangle^i(r,t)$ for $h_{fs} = 66000 W/m^2K$ and for $h_{He} = 30 W/m^2K$

6. REFERENCES

Cotta,R. M. and Mikhailov, M. D., 1997, ”Heat conduction - Lumped analysis, integral transforms, symbolic computation”, John Wiley and Sons, England.

Hsu,C.T.,1999, ”A closure model for transient heat conduction in porous media”, Journal of Heat Transfer, Vol.121, pp. 733-739.

IAEA-TECDOC-1198, Feb 2001, ”Current status and future development of modular high temperature gas cooled reactor technology”, International Atomic Energy Agency, Chapter 2.

IAEA-TECDOC-1382, Nov 2003, ”Evaluation of high temperature gas cooled reactor performance: Benchmark analysis to initial testing of the HTTR and HTR-10”, International Atomic Energy Agency, Chapters 3-4.

Kuwahara, F., Shirota, M. and Nakayama, A., 2001, ”A numerical study of interfacial convective heat transfer coefficient in two-energy equation model for convection in porous media”, International Journal of Heat and Mass Transfer, Vol.44, No.6, pp. 1153-1159.

Miller, G. K., Petti, D. A. and Maki, J. T., 2004, ”Consideration of the effects of partial debonding of the IPyC and particle asphericity on TRISO-coated fuel behavior”, Journal of Nuclear Materials, Vol.334, pp. 79-89.

Miller, G. K., Petti, D. A. and Maki, J. T., 2006, ”An evaluation of the effects of SiC layer thinning on failure of TRISO-coated fuel particles”, Journal of Nuclear Materials, Vol.355 Issues 1-3, pp. 150-162.

Nakayama, A., Kuwahara, F., Sugiyama, M. and Xu, G., 2001, ”A two-energy equation model for conduction and convection in porous media”, International Journal of Heat and Mass Transfer, Vol.44, No. 22, pp. 4375-4379.

Ribeiro, J. W., Cotta, R. M. and Mikhailov, M. D., 1993, ”Integral transform solution of Luikov equations for heat and mass transfer in capillary porous media ”, International Journal of Heat and Mass Transfer, Vol.36, No.18 , pp.4467-4475.

Reitsma,F.,Strydom, G., de Haas, J.B.M., Ivanov, K., Tyobeka, B., Mphahlele, R., Downar, T.J.,Seker, V.,Gougar, H.D., Da Cruz, D.F. and Sikik, U.E., 2006, ”The PBMR steady-state and coupled kinetics core thermalhydraulics benchmark test problems”, Nuclear Engineering and Design, Vol.236, pp. 657-668.

Todreas, N. E. and Kasimi,M. S., 1990,”Nuclear systems I - Thermal hydraulic fundamentals”, Hemisphere Publishing Corporation, Hemisphere Publishing Corporation, New York, USA, pp. 64-67.

Zhang, Z.,Wu, Z., Sun, Y. and Li, F.,2006, ”Design aspects of the Chinese modular high-temperature gas-cooled reactor HTR-PM ”,Nuclear Engineering and Design, Vol.236,No.5-6, pp.485-490.

7. Responsibility notice

The authors are the only responsible for the printed material included in this paper.